GBRV phonon update and JTH/PSlibrary testing

Kevin F. Garrity[*]

National Institute of Standards and Technology,

Gaithersburg, MD 20899

(Dated: April 15, 2015)

Abstract

These notes contain a brief discussion of version 1.4 the GBRV potentials for Quantum Espresso, designed to produce better-converged phonon calculations. In addition, the notes contain testing results on updated versions of the PSlibrary and JTH PAW libraries, which have shown promising performance in tests of single elements. The new testing results indicate a significant improvement in both PSlibrary and JTH since earlier versions of both libraries were tested. The performance of the high precision PSlibrary is comparable to the GBRV results, albeit at a significantly higher plane-wave cutoff. The low precision PSlibrary performs slightly worse at similar cutoffs to the GBRV potentials. The JTH library performs very similarly to the GBRV library in tests of single elements, but it performs worse when testing a few multi-atom compounds, especially those featuring high oxidation states. The GBRV library remains an excellent combination of accuracy and computational efficiency.

These notes are split into two parts. Part I contains phonon convergence results for version 1.4 of the GBRV[1–4] Quantum Espresso[5] pseudopotentials. Part II contains updated testing for the GBRV potentials as well as new versions of the PSlibrary(v1.0.0)[6, 7] and the JTH (v0.2) [8, 9] libraries.

GBRV V1.4

In order to improve the convergence of density functional theory perturbation theory (DFTPT) phonon calculations in Quantum Espresso using the GBRV pseudopotentials[1–4], I have made minor tweaks to the following pseudopotentials: Ag, B, Be, Br, Cl, F, Fe, Ga, Ge, H, In, K, Li, Mg, Na, Ni, Pd, Pt, Rh, Sb, Sn, S, Ti, V, and Y. As seen in the second section, these tweaks, mostly to details of the various core cutoffs and parameters, have very little effect on the structural testing results. These tweaks were designed to improve the convergence of phonon calculations. For a few cases, like K and H, there were significant convergence issues in phonon calculations using previous versions of the pseudopotentials, but in most cases the tweaks just slightly improve the convergence, such that the vast majority are well converged at a plane-wave cutoff of 40 Ryd with a 200 Ryd charge-density cutoff.

To test the convergence, I ran DFTPT phonon calculations at several cutoff energies and compared them to a finite difference phonon calculation performed at a high cutoff. The calculations were done at $q = \Gamma$ for two structures: a conventional *bcc* unit-cell (2 atoms per cell)[14] and a primitive rock-salt structure (also 2 atoms per cell). No LO-TO splitting was included for the insulators. The calculations were done with $10 \times 10 \times 10$ k-point grids and a Fermi-Dirac smearing of 0.015 Ryd. The results are before the acoustic sum rule is enforced, in order to see the deviation of the acoustic modes from zero.

As can be seen in table I, the convergence of the optical modes is very good. Only Li, Be, and B have significant deviation even at the lowest cutoff. The acoustic modes are slower to converge, but this issue (which is typical) is normally fixed by enforcing the acoustic sum rule on the dynamical matrix.

To clarify, in contrast to the following section, this section simply tests convergence, not the accuracy of the pseudopotentials in reproducing all-electron results. In addition, please note that these systems are all very simple, and more complicated systems, especially those

TABLE I: Phonon convergence results, in THz. ω^O_{FD} is the finite difference optical phonon frequency in THz calculated at 60 Ryd PW cutoff and 500 Ryd charge density cutoff. The next three columns ($\Delta\omega^O_{PT}$)are the difference between the finite difference result at high cutoff and the DFT-PT result at three different cutoffs: (40,200), (45,300), (60,500). The final three columns (ω^A_{PT}) are the DFT-PT results for the acoustic modes. The last six columns should ideally all be zero. rs is for rock salt.

Cutoff	ω^O_{FD} (60,500)	$\Delta\omega^O_{PT}$ (40,200)	$\Delta\omega^O_{PT}$ (45,300)	$\Delta\omega^O_{PT}$ (60,500)	ω^A_{PT} (40,200)	ω^A_{PT} (45,300)	ω^A_{PT} (60,500)
Ag *bcc*	4.47	0.00	0.00	0.00	0.50	0.26	0.12
Al *bcc*	8.00	−0.01	0.00	0.00	−0.23	0.17	−0.03
Au *bcc*	3.69	0.00	0.00	0.00	0.16	−0.05	0.11
Ba *bcc*	2.22	0.00	0.00	0.00	−0.07	−0.05	−0.07
B *bcc*	12.30 *i*	0.33	0.12	0.07	2.27	0.44	−0.16
Be *bcc*	19.88	0.10	0.00	0.01	1.99	−0.13	−0.25
Bi *bcc*	0.90	0.00	0.00	0.00	0.09	0.00	−0.03
Ca *bcc*	4.89	0.01	0.01	0.01	−0.09	−0.10	−0.12
C *bcc*	21.24 *i*	0.00	−0.03	−0.04	0.32	0.03	0.06
Cd *bcc*	2.38	−0.01	0.00	0.00	−0.17	−0.06	−0.11
Co *bcc*	7.21	0.00	0.00	0.00	−0.30	0.20	0.28
Cr *bcc*	7.04	−0.02	−0.01	−0.01	0.12	0.20	0.26
Cs *bcc*	0.97	0.00	−0.01	−0.01	−0.07	0.10	0.10
Cu *bcc*	6.95	0.04	0.03	0.01	−0.18	−0.19	−0.10
Fe *bcc*	5.93	0.01	0.00	0.00	−0.09	−0.06	0.21
Ge *bcc*	3.26	0.00	0.00	0.00	−0.13	−0.10	−0.20
Hf *bcc*	3.76	0.03	0.01	0.01	0.62	0.25	−0.24
Ir *bcc*	3.79	−0.01	0.00	0.00	−0.05	0.04	0.01
K *bcc*	2.16	0.00	−0.03	−0.03	−0.17	−0.37	−0.40
La *bcc*	2.10	0.00	0.00	0.00	−0.15	−0.04	−0.08
Li *bcc*	9.98	0.08	0.00	0.01	1.14	−0.57	−0.10
Mg *bcc*	6.93	0.01	−0.01	−0.01	0.26	0.59	0.54
Mn *bcc*	3.13 *i*	0.00	0.00	0.01	0.23	0.24	0.29
Mo *bcc*	4.64	−0.02	0.01	−0.01	0.02	0.19	−0.09
Na *bcc*	3.71	−0.02	−0.02	−0.01	−0.12	0.24	0.30
Nb *bcc*	6.42	0.05	0.01	0.00	0.69	0.23	−0.05
Ni *bcc*	7.85	0.04	−0.01	0.00	0.46	−0.37	0.11
Os *bcc*	4.15	0.00	0.01	0.00	−0.05	−0.04	−0.11
Pb *bcc*	1.59	0.00	0.00	−0.01	−0.11	0.05	−0.15
Pd *bcc*	5.72	0.00	0.00	0.00	0.12	0.11	−0.13
Pt *bcc*	4.29	−0.01	0.00	0.00	0.04	0.07	0.06
Rb *bcc*	1.32	0.00	0.00	−0.02	−0.07	−0.03	0.06
Re *bcc*	1.51	−0.04	−0.04	−0.03	0.05	0.04	−0.10
Rh *bcc*	5.34	−0.01	0.00	0.00	0.09	−0.10	−0.14
Ru *bcc*	4.34	0.02	0.01	0.01	0.08	0.09	−0.18
Sb *bcc*	1.20 *i*	−0.03	−0.03	−0.03	−0.20	−0.26	−0.23

TABLE II: Table I continued.

Cutoff	ω^O_{FD} (60,500)	$\Delta\omega^O_{PT}$ (40,200)	$\Delta\omega^O_{PT}$ (45,300)	$\Delta\omega^O_{PT}$ (60,500)	ω^A_{PT} (40,200)	ω^A_{PT} (45,300)	ω^A_{PT} (60,500)
Sc bcc	6.40	0.00	0.01	0.01	-0.15	0.14	0.13
Si bcc	6.15	0.00	0.00	0.00	0.04	0.11	-0.03
Sn bcc	2.69	0.00	0.00	0.00	0.07	-0.10	-0.10
Sr bcc	3.10	0.00	0.00	0.00	-0.18	-0.13	-0.12
Ta bcc	4.70	0.01	0.00	0.00	0.01	-0.06	-0.07
Tc bcc	3.22 i	0.04	0.04	0.01	-0.07	-0.08	0.06
Ti bcc	6.45	0.03	0.01	0.01	0.08	0.20	-0.06
Tl bcc	1.83	0.00	0.00	0.01	0.11	0.05	0.05
V bcc	7.74	0.00	0.00	0.00	-0.13	-0.10	0.10
W bcc	5.39	-0.01	0.02	0.00	-0.05	0.02	-0.09
Y bcc	4.13	-0.02	0.00	0.00	-0.45	-0.13	-0.10
Zn bcc	4.12	0.00	0.01	0.00	0.11	0.33	0.16
Zr bcc	5.18	0.00	0.00	0.00	-0.09	-0.10	-0.10
GaAl bcc	5.08	0.01	0.02	0.03	-0.22	-0.12	-0.38
InAl bcc	4.70	0.00	0.01	0.01	0.11	0.21	0.18
AlAs rs	5.34	0.00	0.00	0.00	-0.15	-0.05	-0.04
AlBi rs	4.29	0.00	0.00	0.00	-0.08	-0.07	-0.07
AlN rs	13.13	0.00	0.00	0.00	-0.61	-0.23	0.04
AlP rs	6.64	0.00	0.00	0.00	0.20	-0.08	-0.10
AlSb rs	4.61	0.00	0.00	0.00	-0.24	-0.17	-0.22
BeO rs	4.02 i	-0.03	-0.12	0.00	0.23	-0.39	-0.11
BN rs	21.43 i	-0.04	-0.03	0.00	-0.67	-0.59	-0.16
CaO rs	7.57	0.01	0.01	-0.01	-0.16	0.16	0.05
GaN rs	6.40	0.01	0.01	0.00	-0.16	0.17	0.18
HgO rs	5.47	0.00	0.00	0.00	0.02	-0.06	-0.05
InN rs	7.24	0.02	0.02	0.00	0.13	0.13	0.15
LiBr rs	4.15	0.05	0.00	0.00	0.24	-0.08	0.06
LiCl rs	4.94	0.04	-0.06	-0.01	0.37	-0.18	0.23
LiF rs	7.91	-0.02	0.06	0.01	-1.16	0.55	-0.28
LiH rs	17.54	0.06	0.00	0.00	1.25	-0.36	-0.32
LiI rs	3.40	-0.06	-0.03	0.02	0.08	-0.06	0.13
MgO rs	10.90	0.01	0.00	0.00	-0.37	-0.40	-0.26
NaBr rs	3.63	0.01	0.00	-0.01	-0.12	-0.21	-0.27
NaCl rs	4.48	0.00	-0.01	-0.02	-0.18	-0.33	-0.28
NaF rs	6.86	0.03	0.01	0.00	-0.58	-0.26	-0.20
NaI rs	3.08	-0.01	-0.01	-0.01	-0.23	-0.16	-0.25
ScN rs	8.46	0.00	0.01	0.00	-0.04	0.16	0.17
SrO rs	5.62	0.00	0.00	0.00	-0.07	0.09	0.14
SrSe rs	3.79	0.00	0.00	0.00	0.13	0.11	0.12
SrS rs	5.13	0.02	0.00	0.00	0.31	0.08	0.12
SrTe rs	3.30	0.00	0.00	0.00	0.08	0.08	0.10
YN rs	5.00	0.01	0.01	-0.01	0.17	0.08	0.11

with soft phonons, may be more difficult to converge. In addition, all of these results are for non-spin-polarized systems.

The current update is only for the Quantum Espresso USPPs, not the ABINIT[10] PAWs, because the DFTPT+PAW code for ABINIT is still under-development and does not appear to be working at all for GGA, at least in the public version.

NEW TESTING

In this section, I present updated testing results for the GBRV USPP's, as well as the new PSlibrary (v1.0)[6, 7] and JTH (v0.2)[8, 9] PAW libraries. In earlier work, I tested previous versions of these libraries and found that while most of the potentials were good, some of the potentials needed updating in order to improve their transferability.

Both updated potential sets have been tested by their creators in various structures with only a single element, including versus some of the all-electron data originally used to test the GBRV potentials. However, for general-use pseudopotentials, like those intended for high-throughput applications, it is important to test the potentials in a variety possible oxidation states. In my experience, this is an important test of transferability and can reveal issues which are otherwise undetectable.

The JTH PAW potential set is tested with ABINIT at a plane-wave cutoff energy of 40 Ryd and a core cutoff of 100-200 Ryd, which is the same as the GBRV ABINIT potentials.

The PSlibrary set has two versions, a complete high precision set, which requires a high plane-wave cutoff, and an incomplete low precision set which requires a cutoff more comparable to the GBRV set (40 Ryd PW,200 Ryd Charge Density). Here, I present results for the PAW version of the high precision set, which I ran with Quantum Espresso at (100,700). Because of the high cutoff, this potential set is not appropriate for high throughput applications (although the majority of atoms can be run at a lower cutoff). In addition, I tested the low precision PSlibrary set by adding in high precision potentials as need to complete the tests, run at (40,300), a slightly higher charge density cutoff than the GBRV potentials.

Details of the tests are presented in previous work, and the results are in Figures 1-6 and are summarized in table III, as well as older tests[1, 3] of the VASP PAWs[11, 12].

The PSlibrary-high results are very good in all cases, and are at least as good as the GBRV potentials, although as detailed above they are run at a much higher cutoff. The

TABLE III: Summary of pseudopotential testing results. Lattice constant testing data is presented as either RMS errors relative to AE calculations or percent of lattice constants outside $\pm 0.2\%$, Δ-factor is a simple average (smaller is better).

Test	GBRV QE-1.4	GBRV ABINIT	JTH	PSlibrary high	PSlibrary low	VASP
fcc latt. const. (%)	0.14	0.13	0.13	0.14	0.17	0.11
bcc latt. const. (%)	0.15	0.15	0.13	0.14	0.17	0.12
rock salt latt. const. (%)	0.11	0.13	0.42	0.11	0.22	0.15
perovskite latt. const. (%)	0.09	0.09	0.25	0.09	0.22	0.13
half-Heusler latt. const. (%)	0.12	0.13	0.21	0.09	0.13	0.14
zinc blende latt. const. (%)	0.12	0.11	0.43	0.10	0.11	0.11
fcc $> \pm 0.2\%$ (%)	8.2	8.2	11.5	8.2	14.8	8.2
bcc $> \pm 0.2\%$ (%)	8.2	8.2	8.2	8.2	19.7	6.7
rock salt $> \pm 0.2\%$ (%)	11.1	7.9	23.8	9.5	12.7	12.9
perovskite $> \pm 0.2\%$ (%)	1.8	1.8	18.2	3.6	12.7	15.1
half-Heusler $> \pm 0.2\%$ (%)	6.5	6.5	22.4	2.2	15.2	15.7
zinc blende $> \pm 0.2\%$ (%)	3.6	7.1	10.7	5.3	8.9	7.1
zinc blende Δ (meV/atom)	1.2	1.2	1.6	0.9	1.0	1.0
zinc blende Δ_1 (meV/atom)	1.9	2.1	3.2	1.6	1.7	1.8

PSlibrary-low results are mostly very good, but a few elements appear to require higher convergence parameters than the GBRV potentials to reach full accuracy. These results are basically consistent with Ref. [7].

The JTH results are mostly good as well, especially for the elements. The JTH set performs worse than the other sets for some of the high oxidation state compounds. Tl and In in particular are problematic in the (3+) oxidation state, and a few of the transition metals perform worse with non-zero oxidation states.

Overall, the results for all the potential sets are quite promising, and in fact the errors due to the pseudopotentials are already small compared to the systematic errors introduced by the various approximations to the exchange-correlation functional. In many cases, the agreement between the various sets of potentials is good enough that higher quality all-electron results may be necessary to distinguish between them.
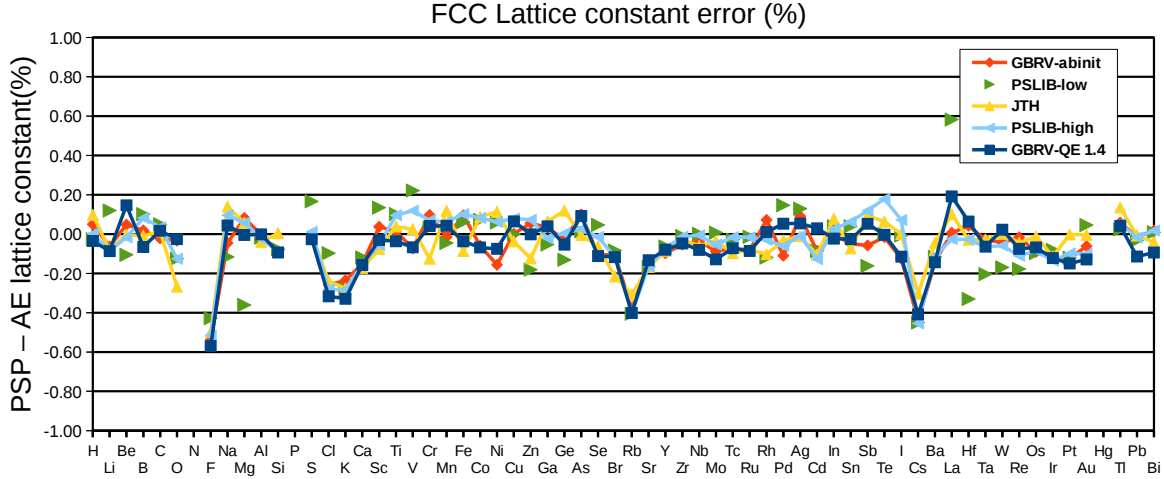
FIG. 1: Percent difference in AE versus pseudopotential calculations for *fcc* lattice constant. GBRV QE USPP results (v1.4) are blue squares, GBRV ABINIT PAW results are red diamonds, JTH results are yellow upward triangles, and PSlibrary-high results are left-pointing cyan triangles, PSlibrary-low results are right-pointing green triangle without a line connecting them.
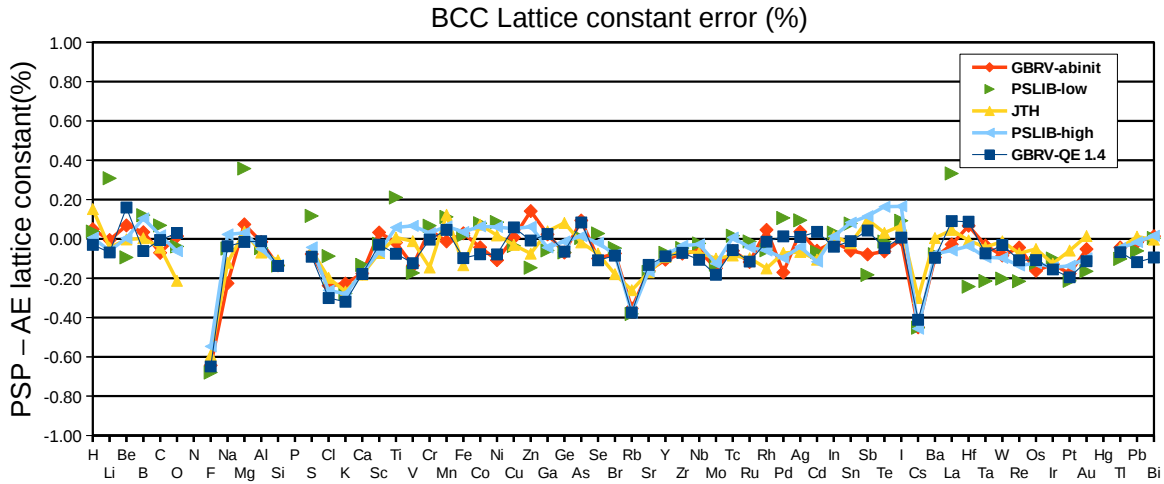

FIG. 2: Percent difference in AE versus pseudopotential calculations for *bcc* lattice constants. Colors as in Fig. 1.

---

* Electronic address: kgarrity@physics.rutgers.edu

[1] K. F. Garrity, J. W. Bennett, K. M. Rabe, and D. Vanderbilt, Comput. Mater. Sci **81**, 446 (2014).

[2] K. F. Garrity, *Notes on abinit gbrv paws* (2013), URL http://www.physics.rutgers.edu/gbrv/notes_on_abinit3.pdf.
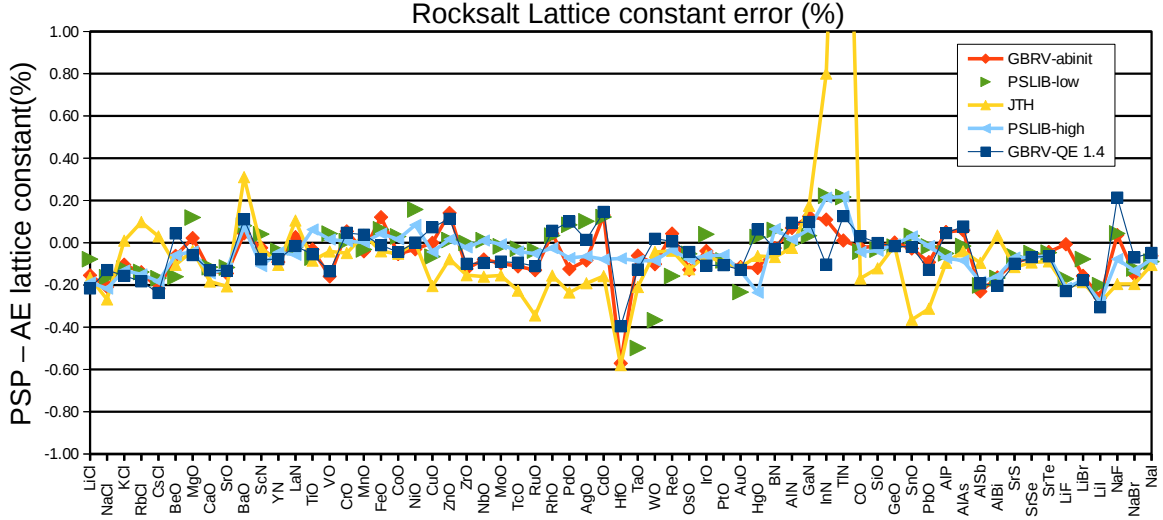
FIG. 3: Percent difference in AE versus pseudopotential calculations for rocksalt lattice constants. HfO is off the scale for PSlib-low (-1.40%). Colors as in Fig. 1.
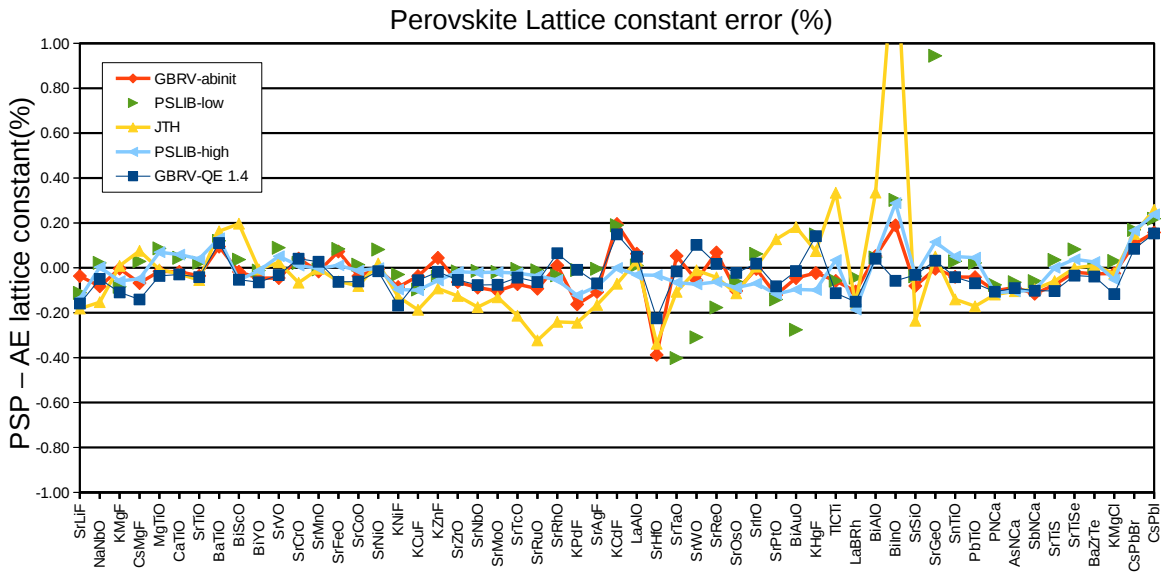

FIG. 4: Percent difference in AE versus pseudopotential calculations for perovskite lattice constants. SrHfO$_3$ is off the scale for PSlib-low (-1.03%). Colors as in Fig. 1.

[3] K. F. Garrity, *Gbrv update and jth testing* (2013), URL http://www.physics.rutgers.edu/gbrv/gbrv_update_jth2.pdf.

[4] K. F. Garrity, J. W. Bennett, K. M. Rabe, and D. Vanderbilt, URL http://physics.rutgers.edu/gbrv.

[5] P. Giannozzi and et al., J. Phys.:Condens. Matter **21**, 395502 (2009).

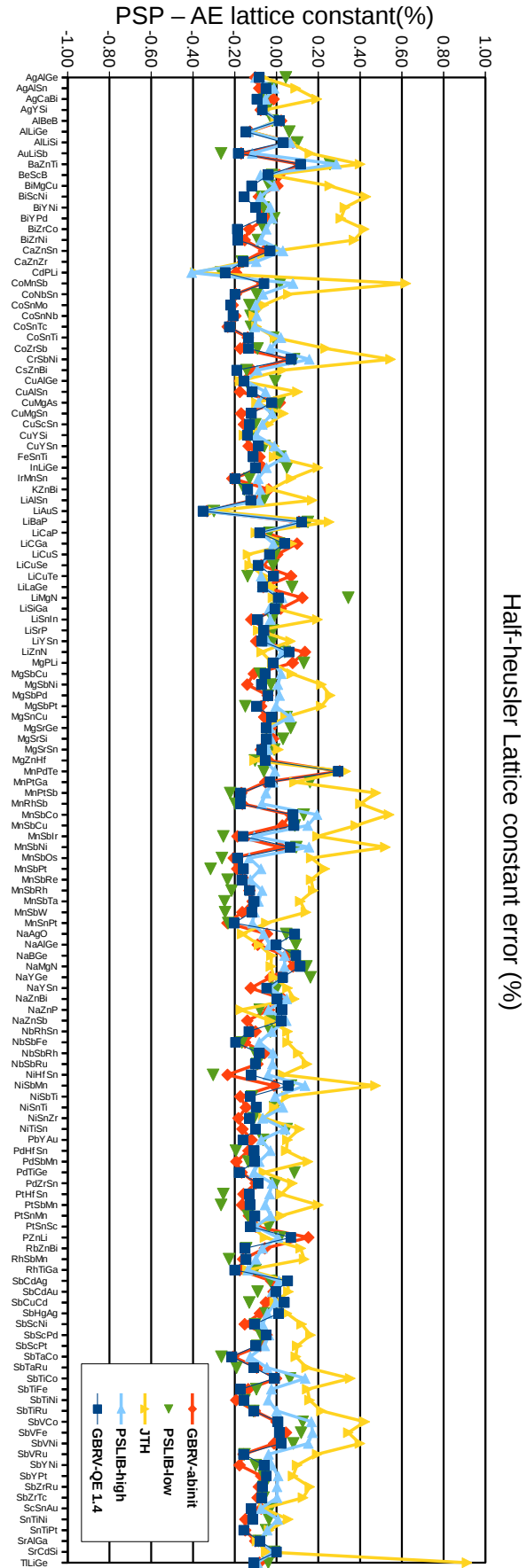[6] http://www.qe-forge.org/gf/project/pslibrary/.

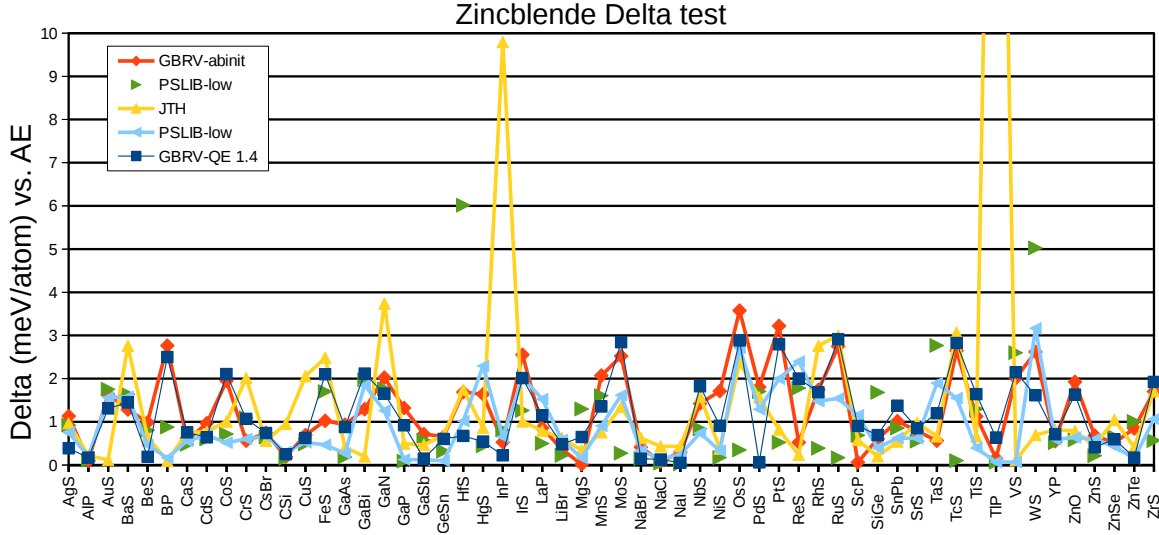FIG. 5: Percent difference in AE versus pseudopotential calculations for half-Heusler lattice constants.

9

FIG. 6: Delta-factor[13] (meV/atom) for AE versus pseudopotential calculations for zinc blende structure. Colors as in Fig. 1.

[7] A. D. Corso, Comput. Mater. Sci. **95**, 337 (2014).

[8] M. T. F. Jollet and N. Holzwarth, Comp. Phys. Comm. **185**, 1246 (2014).

[9] M. T. F. Jollet and N. Holzwarth (2013), URL http://www.abinit.org/downloads/PAW2/.

[10] X. Gonze, G. Rignanese, M. Verstraete, J. Beuken, Y. Pouillon, R. Caracas, F. Jollet, M. Torrent, G. Zerah, M. Mikami, et al., Z. Kristall. **220**, 558 (2005).

[11] G. Kresse and J. Hafner, Phys. Rev. B **47**, R558 (1993).

[12] G. Kresse and J. Furthmuller, Phys. Rev. B **54**, 11169 (1996).

[13] K. Lejaeghere, V. V. Speybroeck, G. V. Oost, and S. Cottenier, Crit. Rev. Solid State Mater. Sci **39**, 1 (2014).

[14] Ga and In had very unstable DFTPT results in the *bcc* structure no matter what I did to the potentials, but worked fine when I replaced half the atoms with Al. I don't really understand why this is, but I think the pseudopotentials are fine. In addition, the optical mode of *bcc* Hg is essentially zero, producing weird results.